Structure and Properties of Composite Films Prepared from Cellulose and Nanocrystalline Titanium Dioxide Particles

Jinping Zhou,*[,1,2] Shilin Liu,[1] Jianing Qi,[1] Lina Zhang[1,3]

[1]*Department of Chemistry, Wuhan University, Wuhan 430072, China*
[2]*Laboratory of Cellulose and Lignocellulosic Chemistry, Guangzhou Institute of Chemistry, Chinese Academy of Sciences, Guangzhou 510650, China*
[3]*Center of Nanoscience and Nanotechnology, Wuhan University, Wuhan 430072, China*

Received 5 January 2005; accepted 8 May 2005
DOI 10.1002/app.22650
Published online in Wiley InterScience (www.interscience.wiley.com).

ABSTRACT: Composite films were successfully prepared from cellulose and two kinds of nanocrystalline TiO_2 particles in a NaOH/urea aqueous solution (7.5 : 11 in wt %) by coagulation with H_2SO_4 solution. The structure, morphology, and properties of the films were characterized by transmission electron microscopy, scanning electron microscopy, X-ray diffraction, TGA, tensile testing, UV–vis spectroscopy, and antibacterial test. The results indicated that TiO_2 particles in a cellulose matrix maintained the original nanocrystalline structure and properties. TiO_2(I) (anatase) and TiO_2(II) (the mixture of anatase and rutile) particles exhibited a certain miscibility with cellulose. The tensile strength of two kinds of composite films was higher than 70 and 75 MPa, when the content of TiO_2(I) and TiO_2(II) was 4 and 11 wt %, respectively. The cellulose composite films containing nanocrystalline TiO_2 particles displayed distinct antibacterial abilities and excellent UV absorption. This work provides a potential way for preparing functional composite materials from cellulose and inorganic nanoparticles in a NaOH/urea aqueous solution, without a destruction of the structure and properties of the particles. © 2006 Wiley Periodicals, Inc. J Appl Polym Sci 101: 3600–3608, 2006

Key words: cellulose; nanocrystalline TiO_2 particles; composites; films; structure

INTRODUCTION

Recently, polymer–inorganic nanoparticle composite materials have attracted the interest of a number of researchers, due to their synergistic and hybrid properties derived from individual components.[1–3] Titanium dioxide (TiO_2), as a cheap and nontoxic material, has been largely used in technical applications as a white pigment for paints or cosmetics, a support in catalysis, and photocatalyst.[4,5] Through a combination of the superiority of polymer and nanocrystalline TiO_2 particles, a variety of polymer–TiO_2 hybrid nanocompositess with unique optical, photocatalystic, and electrical properties have been reported in the literatures.[6–12]

Cellulose is one of the most abundant naturally occurring polymers in the world, which can be regenerated or derivatized to yield various useful products as a result of its renewability, biodegradability, biocompatibility, and derivatizability.[13] However, only a few nanocomposite functional materials based on cellulose have been reported, because cellulose cannot be dissolved in common solvent. Kunitake et al. provided a simple route to manufacturing of noble metal (Ag, Au, Pt, Pd) nanoparticles by using porous natural cellulose fibers as nanoreactor and particle stabilizer.[14] Cellulose acetate films containing iron and copper nanoparticles have demonstrated catalytic activities in hydrogenation of olefins, CO oxidation, NO reduction, and water–gas shift reaction.[15,16] Park et al. have reported the antimicrobial ultrafine cellulose acetate fibers with silver nanoparticles too.[17] In previous work, we have developed two kinds of novel solvent for cellulose, namely NaOH/urea and NaOH/thiourea aqueous solution,[18,19] and the regenerated cellulose films and fibers with excellent mechanical properties have been successfully prepared.[20–22] Moreover, antibacterial regenerated cellulose/tourmaline nanocrystal composite films have been prepared in NaOH/thiourea aqueous solution.[23] To expand the functionality of cellulose, composite films from cellulose and two kinds of nanocrystalline TiO_2 particles were prepared in NaOH/urea aqueous solution in this work, and the structure, morphology, and properties of the films were characterized.

*Correspondence to: J. Zhou (jp.zhou@263.net).
Contract grant sponsor: National High Technology Research and Development Program of China (863 Program); contract grant numbers: 2003AA333040, 2004AA649250.
Contract grant sponsor: National Natural Science Foundation of China; contract grant numbers: 20204011.
Contract grant sponsor: Foundation of Key Laboratory of Cellulose and Lignocellulosic Chemistry, Chinese Academy of Sciences, China.

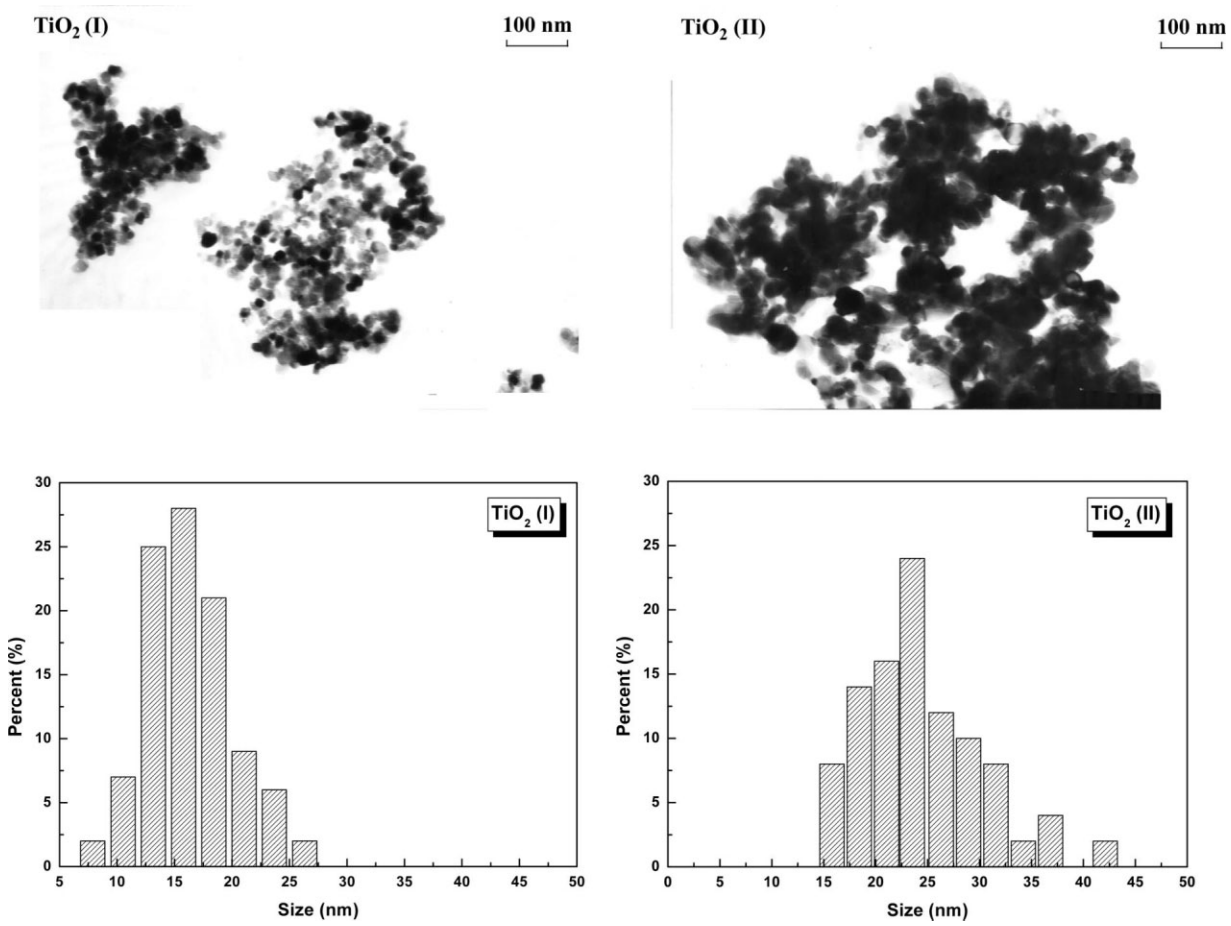

Figure 1 TEM images (top) and size distribution (bottom) of the nanocrystalline TiO_2 particles.

EXPERIMENTAL

Materials

Cellulose (cotton linters pulp) was purchased from Hubei Chemical Fiber Group, Ltd. (China), and the viscosity–average molecular weight of the linters in cadoxen at 25°C was determined to be 10.3×10^4 by viscometry according to $[\eta]$ (mL/g) = $3.85 \times 10^{-2} M_w^{0.76}$.[24]

Two kinds of nanocrystalline TiO_2 particles, coded as TiO_2(I) (anatase type, BET 71 m^2/g) and TiO_2(II) (the mixture of anatase and rutile types, BET 55 m^2/g), were provided by the Chemical Factory of Wuhan University. Figure 1 shows the transmission electron microscopy (TEM) images and size distribution of the nanocrystalline TiO_2 particles. Two kinds of TiO_2 particles mainly exist in an agglomeration state, and TiO_2(II) displays larger mean size and broader distribution than TiO_2(I), and the mean size of TiO_2(I) and TiO_2(II) are determined to be 16 and 30 nm, respectively.

Beef extract, agar, and peptone broth were of biological reagent grade. All of the other solvents and chemicals used in this work are analytic reagent grade and used without further purification.

Preparation of composite films

A desired amount of nanocrystalline TiO_2 particles were dispersed into a flask containing 200 g NaOH/urea aqueous solution (7.5:11 in wt %), and the solution was stirred by mechanical stirring at room temperature for 12 h, then the suspension solution was cooled down to −12°C. Cellulose (8.2 g) was dripped immediately into the precooled NaOH/urea aqueous solution containing TiO_2 particles and stirred vigorously by mechanical stirring at room temperature. The resulting mixture solution was subjected to centrifugation at 10,000 rpm for 15 min at 10°C to exclude a few gels (<5 wt %) and to carry out the degasification. The mixture solution was poured into a glass plate to a thickness of 0.5 mm and was immediately immersed in a 5.6 wt % H_2SO_4 aqueous solution for 5 min to coagulate. The resulting composite film was washed with running water and dried in the air. By changing the amount of TiO_2 in the solution, the composite films containing TiO_2(I) and TiO_2(II) with different weight percent (as listed in Table I) were prepared and coded as CA and CT series, respectively. The RC films were prepared from pure cellulose in the NaOH/urea aqueous solution, according to the same method.

TABLE I
The Content of Nanocrysatalline TiO_2 Particles in the Composites Films[sr1]

Code number	TiO_2 (I) content (%)	Code number	TiO_2 (II) content (%)
CA-1	0.25	CT-1	1.17
CA-2	1.27	CT-2	2.16
CA-3	1.53	CT-3	3.39
CA-4	2.61	CT-4	5.41
CA-5	3.23	CT-5	7
CA-6	4.05	CT-6	11.17

Characterization

The Brunauer-Emmett-Teller (BET) surface area of TiO_2(I) and TiO_2(II) were obtained with nitrogen adsorption in a Beckman Coulter surface area analyzer (SA 3100, Beckman). Scanning electron microscopy (SEM) was carried out on a Hitachi S-570 scanning electron microscope (Hitachi, Ibaraki, Japan). The films were sputtered with gold and then observed and recorded. TEM was performed with a Hitachi H-600 electron microscope (Hitachi, Ibaraki, Japan). The composite films were embedded in an epoxy resin. Ultrathin sections were obtained via sectioning on an LKB-8800 ultraome. The TiO_2 nanoparticles were dispersed with ultrasonic in ethanol for 20 min, and then were supported by copper silkscreen for observation. The light transmittance of the films was measured with a Shimadzu UV-160A spectroscope (Shimadzu, Kyoto, Japan) at the wavelength from 200 to 1000 nm, and the thickness of the films were about 30 μm.

The composite films were cut into particle-like size and then vacuum-dried for 24 h before the measurements of thermogravimetry analysis (TGA) and X-ray diffraction (XRD). TGA of the films was measured using a Netzsch TG209 thermal analyzer (Bayern, Germany), with a heating rate of 20°C/min from 30 to 800°C under a nitrogen atmosphere. The XRD of nanocrystalline TiO_2 particles and the composite films were carried out in an X-ray diffractometer (D/MAX-1200, Rigaku Denki, Japan). XRD patterns with Cu Kα radiation (1.5406×10^{-10} m) at 40 kV and 30 mA were recorded in the range of $2\theta = 4-80°$. The degree of crystallinity (χ_c) was calculated according to the usual method.[25] Apparent crystal size (ACS) was estimated through Scherrer's equation:[26]

$$\mathrm{ACS} = \frac{k\lambda}{(\cos\theta)\beta} \tag{1}$$

$$\beta = (B^2 - b^2)^{1/2} \tag{2}$$

where k is the apparatus constant, and taken as 0.89, λ is the wavelength of Cu Kα line (1.5406×10^{-10} m), θ is the Bragg's angle, b the instrumental constant (0.1°), and B is the half width in radians of the diffraction peak of the (101) planes of anatase and (110) planes of rutile for TiO_2. The anatase content A was determined as weight percentage by using the following equation:[27]

$$A = \frac{100}{1 + 0.105 + 0.437F} \tag{3}$$

where F represents the ratio of the integrated area of the rutile and the anatase diffraction peaks.

The tensile strength (σ_b) and elongation at break (ε_b) of the composite films in dry and wet states were measured on a universal tensile tester (CMT6503, Shenzhen SANS Test Machine Co, Ltd, China), according to ISO6293–1986 (E) at a speed of 20 mm/min and 5 mm/min, respectively. The wet films were measured immediately after soaking in water for 30 min.

Antibacterial test

Culture medium was prepared according to the following: 10 g of peptone broth, 5 g of beef extract, and 5 g of NaCl were dissolved in 1000 mL of distilled water by heating, the pH of the solution was adjusted to 7.0–7.2 by NaOH aqueous solution, and then 20 g of agar was added and heated to dissolve completely. Phosphate buffer solution (PBS) was prepared as the following: 72 mL of Na_2HPO_4 (0.2 mol/L) aqueous solution and 28 mL of NaH_2PO_4 (0.2 mol/L) aqueous solution were added into 1000 mL of distilled water, and then 5 g NaCl was added into the mixture solution. The culture medium and PBS used for the anti-

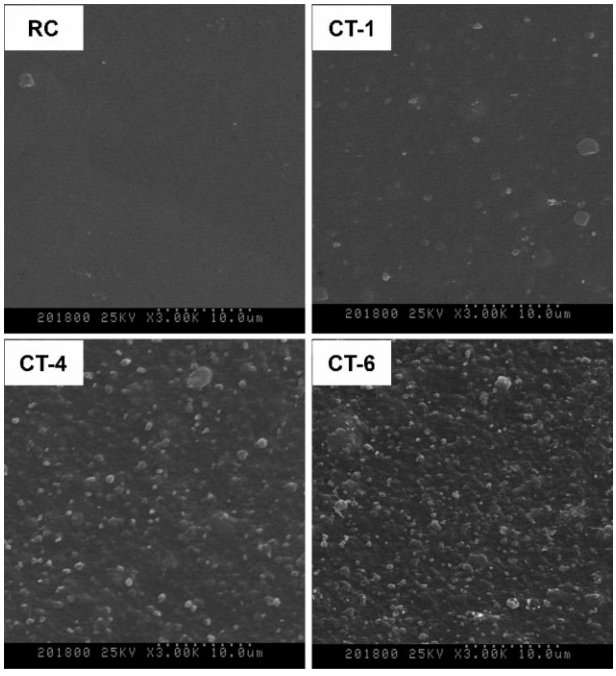

Figure 2 SEM images of the surface of the RC and the composite films (CT series).

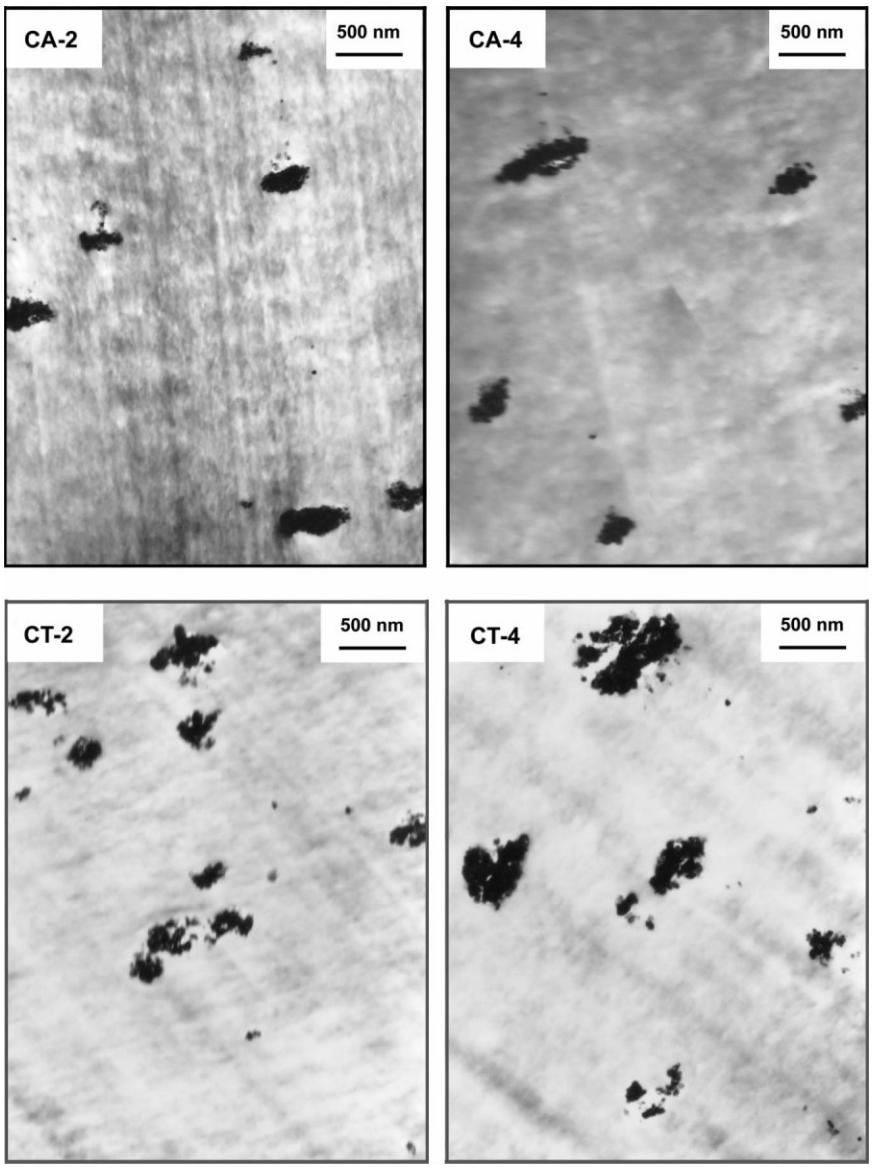

Figure 3 TEM images of the composite films.

bacterial assay were sterilized at 120°C in an autoclave for 20 min. A typical bacteria, *Staphylococcus aureus* (*S. aureus*), for the antibacterial activity evaluation of materials was supplied by the Chinese Center for Type Culture Collection at Wuhan University. The RC and CA composite films (1 cm × 4 cm) were covered on the culture medium and sterilized in the UV light for about 30 min. Bacterial broth culture (10 μL) was seeded onto the films and incubated at 37°C for 24 h, and then all samples were deposited directly under sunlight for 2 h.The films were placed into test tubes containing 10 mL PBS and extensively shaked to fully wash down the bacterial colony. Subsequently, 10 μL of the solution taken out from each tube was seeded onto the culture medium and incubated at 37°C for 24 h. Finally, the units of colony formation in each agar plate were observed to examine the antibacterial ability of each film.

RESULTS AND DISCUSSION

Structure and morphology of composite films

Figure 2 shows the SEM images of the surface of the RC and the CT composite films. The RC film displayed a smooth and dense surface structure. With the addition of nanocrystalline TiO_2(II) particles, the surface of the composite films become more and more rough. Obviously, the agglomerates of nanocrystalline TiO_2 with the mean size about 500 nm dispersed homogenously on the cellulose bed, and the particle numbers increased with an increase of TiO_2 content, indicating some extent of miscibility between cellulose and TiO_2 particles.

Figure 3 shows the TEM images of the composite films. Similar to the pure nanoparticles dispersed in ethanol, TiO_2 particles displayed strong aggregation and an inhomogeneous dispersion in the composites.

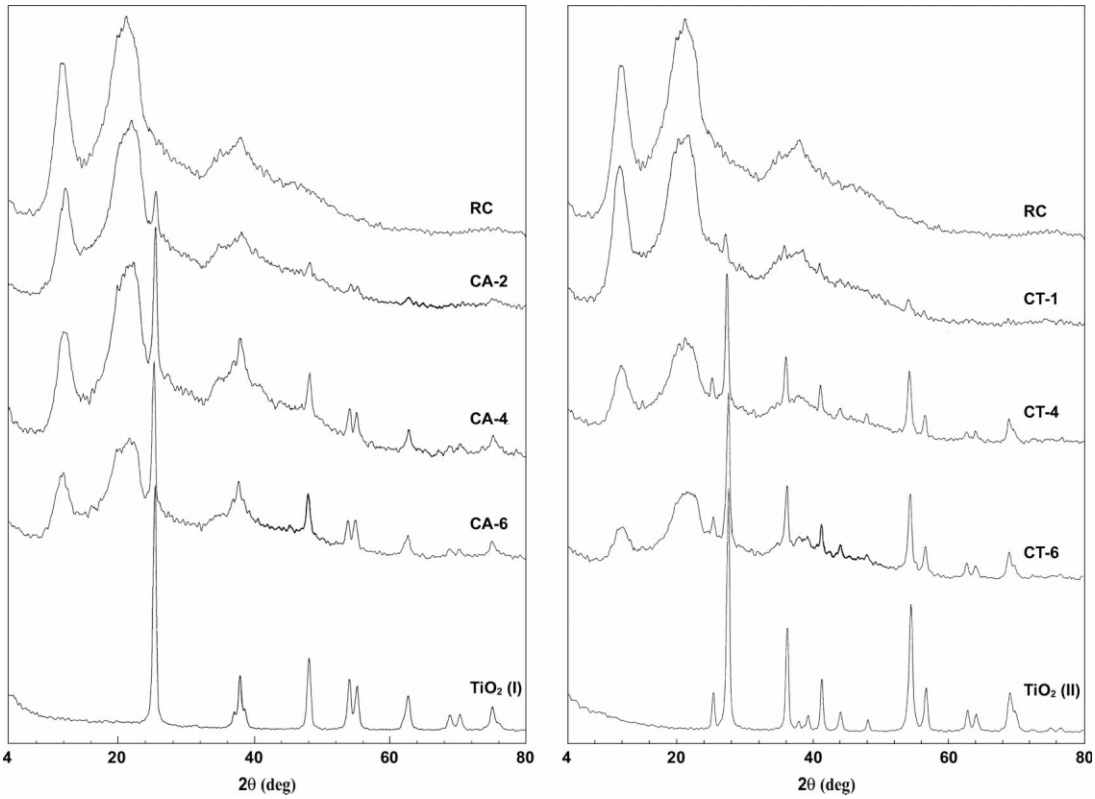

Figure 4 XRD patterns of the nanocrystalline TiO_2 particles, RC, and the composite films.

With an increase of TiO_2 content, the slightly larger aggregation domains exhibit in the films. However, the mean size of nanoparticles nearly unchanged in the composite films, and no cracks or voids could be observed between the interface of cellulose and TiO_2 particles. Therefore, this is a potential system for the preparation of composites from cellulose and nanoinorganic particles in NaOH/urea aqueous solution.

The XRD patterns of the nanocrystalline TiO_2 particles, the RC film, and the composite films are shown in Figure 4. The diffraction peaks were observed at $2\theta = 25.3°$, 37.8°, and 48.4° for TiO_2(I) and $2\theta = 25.3°$, 27.2°, 36.1°, 37.8°, 39.3°, and 48.4° for TiO_2(II). This indicated a mixture of two polymorphs of TiO_2 in TiO_2(II) (anatase and rutile), but only pure anatase for TiO_2(I).[28] The anatase and rutile content of the TiO_2(II) particles was calculated with eq. (3) and was found to be 30 and 70%, respectively. The RC films have characteristic diffraction peaks at $2\theta = 12°$, 20°, and 22° corresponding to (110), (110), and (200) planes of Cellulose II, respectively.[29] For the CA and CT composite films, except for the diffraction peaks of RC, the peaks all correspond to their pure nanocrystalline TiO_2 particles, indicating that the crystals of TiO_2 unchanged in the composites. ACS of (101) planes in anatase and (110) planes in rutile of TiO_2(I) and TiO_2(II) in their composite films are summarized in Table II. The average ACS values of (101) planes in anatase of TiO_2(I) in the CA composite films are determined to be 16 nm, and the values of (101) planes in anatase and (110)

TABLE II
The Crystal Characters of the Nanocrystalline TiO_2 Particles and the Composite Films[sr2]

Sample	Total χ_c (%)	χ_c for cellulose (%)	ACS (nm) (101) in anatase	Sample	Total χ_c (%)	χ_c for cellulose (%)	ACS (nm) (101) in anatase	ACS (nm) (110) in rutile
RC	46	46						
CA-1	47	46	—	CT-1	51	49	—	16
CA-2	50	44	16	CT-2	53	48	—	16
CA-3	52	43	16	CT-3	55	47	16	14
CA-4	54	43	16	CT-4	57	44	16	14
CA-5	56	42	16	CT-5	60	40	16	16
CA-6	59	38	16	CT-6	63	36	16	16
TiO_2(I)			16	TiO_2(II)			16	14

planes in rutile of TiO_2(II) in the CT composites are determined to be 16 nm and 14–16 nm, respectively. The results are similar to the values of their pure nanoparticles, suggesting that the dimension of the TiO_2 particles does not grow up in the composite films. The different mean size of TiO_2(II) observed by XRD and TEM can be assigned to the different measure mode, and the particles observed by TEM are the aggregates of anatase and ruitiles phases. Table II lists the total χ_c values for the composite films and the χ_c values for cellulose (deduct from the effects of nanocrystalline TiO_2 particles) in the composites. The χ_c values for cellulose in the CA composites decrease with an increase of the TiO_2(I) content; but those of the CT composites slightly increase when the TiO_2(II) content was less than 4%, and then decrease with the further addition of particles. This suggests that the crystalline behavior of cellulose could be partially destroyed with the introduce of nanoparticles for a strong interface interaction between cellulose and TiO_2, and the effect of TiO_2(I) is larger than that of TiO_2(II) can be attributed to the smaller particle size and higher BET values of the former. However, the total χ_c values of the composite films increase with increasing TiO_2 content, because of the attribution of nanocrystalline particles, which still maintaining its crystal structure as illustrated in Figure 4. NaOH/urea and NaOH/thiourea aqueous solutions are nonderivative solvents of cellulose,[20,30,31] which cannot destroy the structure of the inorganic additives, such as TiO_2 and tourmaline nanocrystal particles.[23] Therefore, it provided a novel method for preparing functional cellulose composite materials containing inorganic particles with the original structure and character.

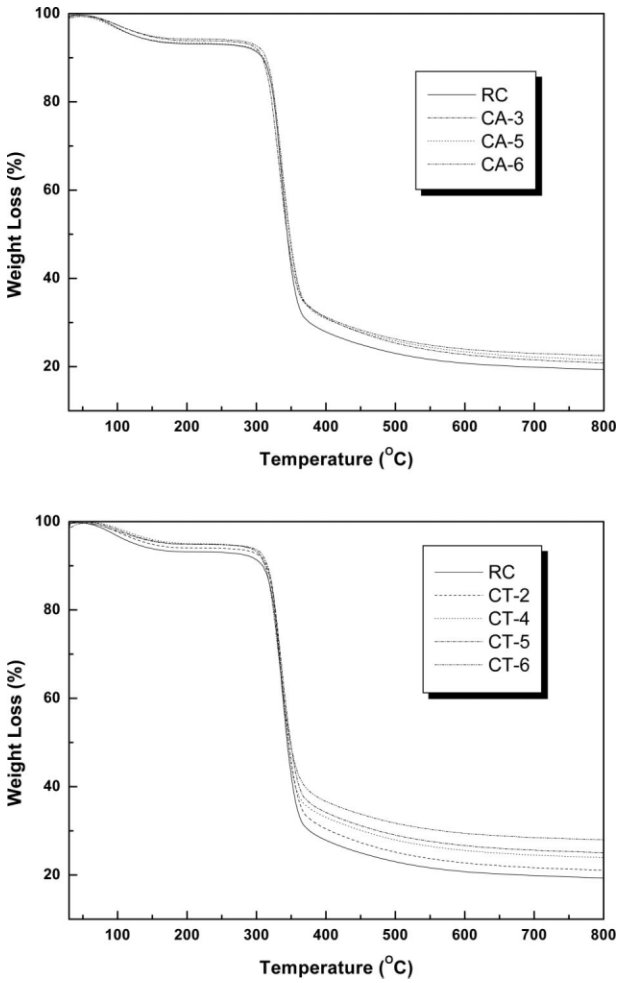

Figure 5 TGA curves of the RC film and the CA and CT composite films.

Properties of composite films

Thermal degradation patterns of the RC and the composite films are shown in Figure 5. The composite films have a thermal degradation pattern that is similar to that of the RC film. A small weight loss of about 5–10 wt % at 50–120°C could be assigned to the release of moisture from the samples. The greatest weight loss found in the temperature range of 300–400°C for RC and the composite films is attributed to the decomposition of cellulose. The amount of the thermal degradation residues of the composites increases with an increase of TiO_2 content. The results indicate that the introduction of nanocrystalline TiO_2 in cellulose films does not reduce the thermal stability, and suggest some extent of miscibility between cellulose and the inorganic particles.

Figures 6 and 7 show the dependence of σ_b and ε_b on the TiO_2 content of the composite films in the wet and dry states, respectively. The values of σ_b and ε_b of the CA composite films in the wet and dry states decrease with an increase of TiO_2(I) content. Just as happens with the CA composite films, the values of σ_b and ε_b of the CT composite films in the dry state slightly decrease with increasing TiO_2(II) content, but the σ_b and ε_b values in the wet state hardly changed. Moreover, the σ_b values of the CT films are higher than those of CA films with the similar content of TiO_2 particles. As shown in the TEM images of the composite films, TiO_2 particles aggregated strongly and dispersed inhomogeneously in the composite films, which partly destroyed the mesh structure of cellulose and resulted in the decrease of mechanical properties. However, the tensile strength of the CA and CT composite films is still higher than 70 and 75 MPa when the TiO_2 content is higher than 4 and 11 wt %, respectively, suggesting a promising practical applicability.

TiO_2 particles in rutile have good UV-blocking power and have already been used as UV absorbers in polymeric composites.[12,32] The UV–vis absorption spectra of the CT and RC films are shown in Figure 8. With the addition of TiO_2 particles, the light transmittance of the composite films decrease and display strong absorption for UV. The UV absorption of the composite films shifts to visible light region with an

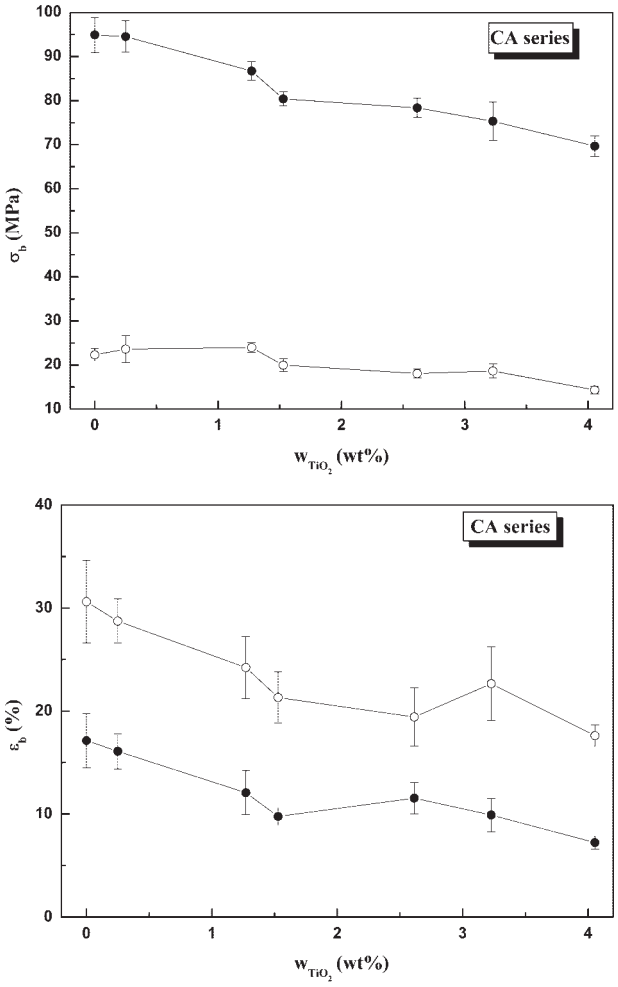

Figure 6 TiO_2(I) content (w_{TiO_2}) dependence on the tensile strength (σ_b) and elongation at break (ε_b) of the composite films (CA series) in dry (●) and wet (○) states.

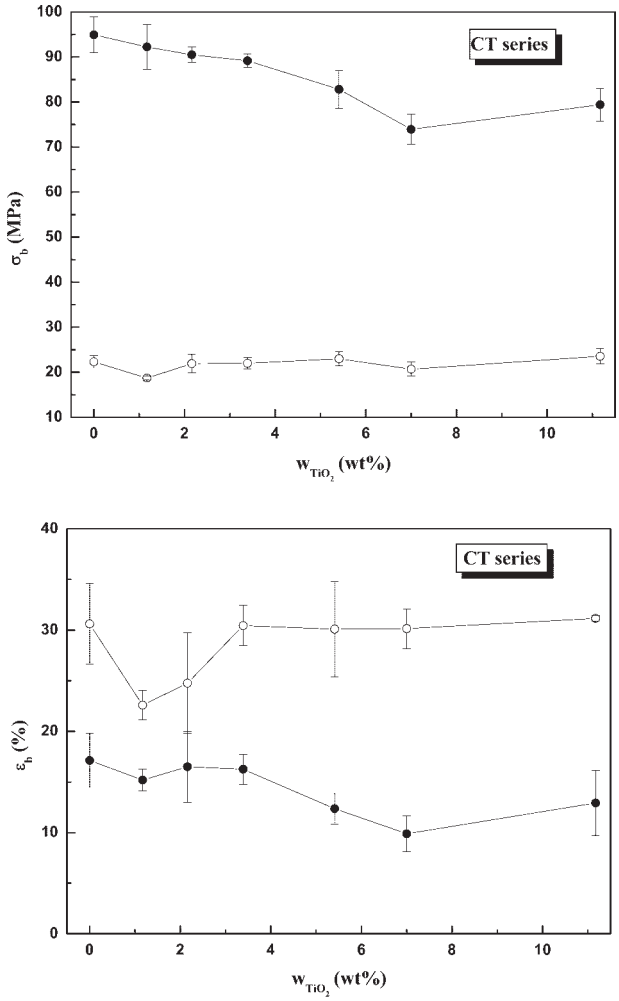

Figure 7 TiO_2(II) content (w_{TiO_2}) dependence on the tensile strength (σ_b) and elongation at break (ε_b) of the composite films (CT series) in dry (●) and wet (○) states.

increase of the TiO_2 content. This indicates that the regenerated cellulose/nanocrystalline TiO_2 composite film was an excellent UV absorption material.

Figure 9 shows the *S. aureus* inoculated on the films RC and CA-4 before the sunlight irradiation (under the dark condition) and after irradiation by sunlight for 2 h. Under the dark condition, the antibacterial activity of the composite film CA-4 is indistinct compared with RC film. It is noted that composite film CA-4 displayed excellent antibacterial activity against *S. aureus* after irradiation by sunlight for 2 h; all of the bacterial colonies on the film have been killed. Except the film CA-1, similar antibacterial activity can be observed for the other CA films. Nanocrystalline TiO_2 particles in anatase have an excellent photocatalytic ability to break down organisms and bacteria even under indoor room lighting conditions.[33] This result further proved, the conclusion mentioned previously, that TiO_2 particles in composite films maintain the original structure and function. Cellulose is a favorite undergarment material because of its high tensile strength, safety, and comfort for the human body. The excellent antibacterial activities of the composite films may lead to applications in the fields of health-protection textiles and food package films.

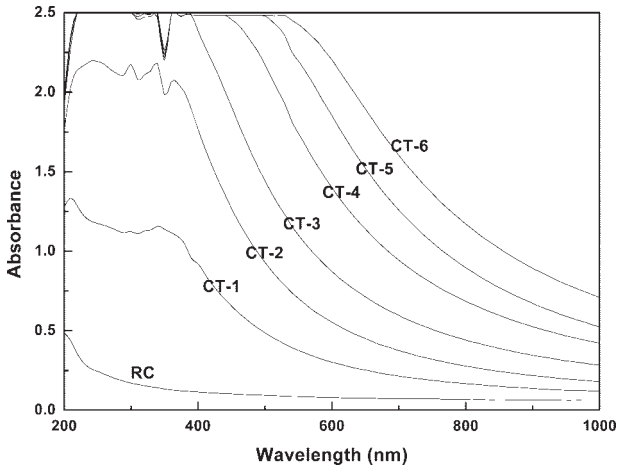

Figure 8 The UV–vis absorbance curves of the RC and CT composite films.

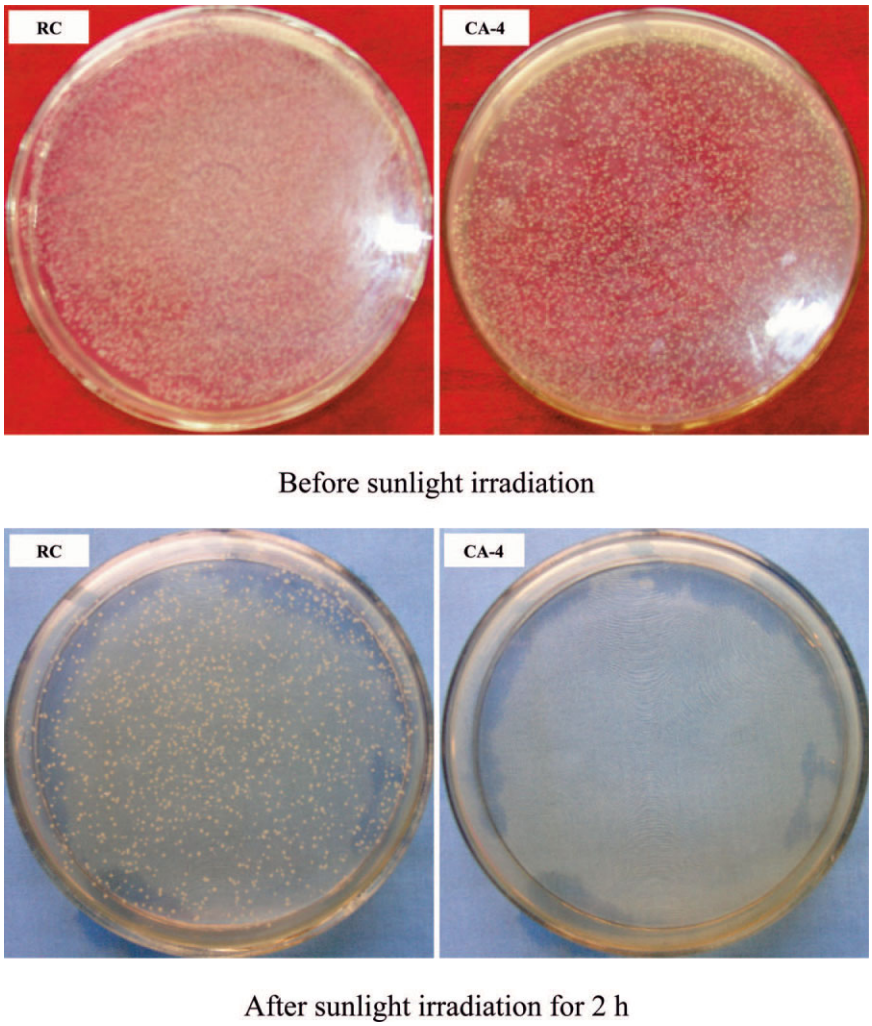

Figure 9 Antibacterial activities of the RC and CA-4 composite films against *S. aureus*.[Color figure can be viewed in the online issue, which is available at www.interscience.wiley.com.]

CONCLUSIONS

Two kinds of regenerated cellulose/nanocrystalline TiO_2 particles composite films were successfully prepared from a NaOH/urea aqueous solution (7.5:11 in wt %) by coagulating with H_2SO_4 solution. The results indicated that TiO_2 particles maintaining the original nanocrystalline structure and properties, dispersed inhomogeneous in the cellulose matrix. The tensile strength of the composite films slightly decreased with an increase of TiO_2 content. However, the σ_b of the CA and CT composite films was higher than 70 and 75 MPa, when the content of TiO_2(I) and TiO_2(II) was 4 and 11 wt %, respectively. The cellulose composite films prepared from TiO_2(I) displayed distinct antibacterial abilities, whereas the composites with TiO_2(II) exhibited excellent UV absorption. The composite films not only maintained the excellent tensile strength of the cellulose films but also kept the structure character and function of nanocrystalline TiO_2 particles. This work provides a potential way for preparing functional composite materials from cellulose and inorganic nanoparticles in NaOH/urea aqueous solutions.

References

1. Ishida, H.; Campbell, S.; Blackwell, J. Chem Mater 2000, 12, 1260.
2. Xiong, H.; Zhao, X.; Chen, J. J Phys Chem B 2001, 105, 10169.
3. Schmidt, G.; Malwitz, M. M. Curr Opin Colloid Interface Sci 2003, 8, 103.
4. Wang, R.; Hasimoto, K.; Fujishima, A. Nature 1997, 388, 431.
5. Mandelbaum, P. A.; Regazzoni, A. E.; Blesa M. A.; Bilmes, S. A. J Phys Chem B 1999, 103, 5505.
6. Wang, B.; Wilkes, G. L.; Hedrick, J. C.; Liptak, S. C.; McGrath, J. E. Macromolecules 1991, 24, 3449.
7. Liu, Y.; Wang, A.; Claus, R. J Phys Chem B 1997, 101, 1385.
8. Zhang, J.; Luo, S.; Cui, L. J Mater Sci 1997, 32, 1469.
9. Lee, L. H.; Chen, W. C. Chem Mater 2001, 13, 1137.
10. Zhang, J.; Ju, X.; Wang, B.; Li, Q.; Liu, T.; Hu, T. Synthetic Met 2001, 118, 181.
11. Yuwono, A. H.; Xue, J.; Wang, J.; Elim, H. I.; Ji, W.; Li, Y.; White, T. J. J Mater Chem 2003, 13, 1475.
12. Nussbaumer, R. J.; Caseri, W. R.; Smith, P.; Tervoort, T. Macromol Mater Eng 2003, 288, 44.

13. Schurz, J. Prog Polym Sci 1999, 24, 481.
14. He, J.; Kunitake, T.; Nakao, A. Chem Mater 2003, 15, 4401.
15. Shim, I. W.; Choi. S.; Noh, W. T.; Kwon, J.; Cho, J. Y.; Chae, D. Y.; Kim, K. S. Bull Korean Chem Soc 2001, 22, 772.
16. Shim, I. W.; Noh, W. T.; Kwon, J.; Cho, J. Y.; Kim, K. S.; Kang, D. H. Bull Korean Chem Soc 2002, 23, 563.
17. Son, W. K.; Youk, J. H.; Lee, T. S.; Park, W. H. Macromol Rapid Commun 2004, 25, 1632.
18. Zhang, L.; Zhou, J. Chinese Pat. ZL00114486.3 (2003).
19. Zhang, L.; Ruan, D.; Gao, S. Chinese Pat. ZL00128162.3 (2003).
20. Zhang, L.; Ruan, D.; Zhou, J. Ind Eng Chem Res 2001, 40, 5923.
21. Cai, J.; Zhang, L.; Zhou, J.; Jin, H.; Chen, H. Macromol Rapid Commun 2004, 25, 1558.
22. Ruan, D.; Zhang, L.; Zhou, J.; Jin, H.; Chen, H. Macromol Biosci 2004, 4, 1105.
23. Ruan, D.; Zhang, L.; Zhang, Z.; Xia, X. J Polym Sci Part B: Polym Phys 2004, 42, 367.
24. Brown, W.; Wiskston, R. Eur Polym J 1965, 1, 1.
25. Rabek, J. F. Experimental Methods in Polymer Chemistry: Applications of Wide-Angle X-Ray Diffraction (WAXS) to the Study of the Structure of Polymers; Wiley: Chichester,UK, 1980; p 505.
26. Scherrer, G. N. Gottinger Nachr 1918, 2, 98.
27. Spurr, R. A.; Myers, H. Anal Chem 1957, 29, 760.
28. Han, H.; Zan, L.; Zhong, J.; Zhang, L.; Zhao, X. Mater Sci Technol B 2004, 110, 227.
29. Marchessault, R.; Sundarajan, P. In The Polysaccharides; Aspinal, G., Ed.; Academic Press: New York, 1985; Vol. 2, p 11.
30. Zhou, J.; Zhang, L.; Cai, J. J Polym Sci Part B: Polym Phys 2004, 42, 347.
31. Zhang, L.; Ruan, D.; Gao, S. J Polym Sci Part B: Polym Phys 2002, 40, 1521.
32. Yang, H.; Zhu, S.; Pan, N. J Appl Polym Sci 2004, 92, 3201.
33. Fujishima, A.; Hashimoto, K.; Yoshinobu, K. Hyomen Kagaku 1995, 16, 188.